Controlling Biofilm Growth and Its Antibiotic Resistance in Drinking Water by Combined UV and Chlorination Processes

Yiwei Chen [1,†] , Yizhen Li [2,3,†] , Shaolun Yang [2], Tsung Yen Chiang [2], Xiaoying Zhu [3] and Jiangyong Hu [1,2,*]

1   NUS Environmental Research Institute, National University of Singapore, 5A Engineering Drive 1, Singapore 117411, Singapore
2   Department of Civil & Environmental Engineering, National University of Singapore, 1 Engineering Drive 2, Singapore 117576, Singapore
3   Department of Environmental Science, Zhejiang University, Hangzhou 310058, China
*   Correspondence: ceehujy@nus.edu.sg
†   These authors contributed equally to this work.

Abstract: Combined use of light-emitting diodes (LED) ultraviolet (UV) and chlorination provides alternative disinfection in drinking water, which could affect the biofilm formed subsequently. Two sequential integrations (UV-Cl and Cl-UV) and one simultaneous combination (UV/Cl) were adopted to investigate their impacts on biofilm formation. Natural organic matter after combined processes was more accessible for microbes. This might explain the promoted growth of culturable biofilm bacteria—biofilm bacteria stabilized at 10^4 CFU/mL without disinfection while increasing continuously to 10^5 CFU/mL in 106 days after combined processes. Contrarily, the viable biofilm bacteria were efficiently suppressed by combined processes, with the least bacteria observed in UV/Cl. The culturable ciprofloxacin-resistant bacteria in biofilm was suppressed by combined processes, with the survival reduced from 49.9% in the control to 27.7%, 16.0% and 10.8% in UV-Cl, Cl-UV and UV/Cl, respectively. The survival of sulfamethoxazole/trimethoprim-resistant bacteria was lower in UV/Cl (16.8%) than others (43.6–55.0%), consistent with the little *sul1* and *sul2* detected in UV/Cl. Although combined processes reduced most detected antibiotic resistance genes (i.e., *blaTEM-1*, *tetA*, *sul1* and *sul2*), UV-Cl showed the potential to enrich *tetA* and *sul2* in biofilm. Overall, UV/Cl outperformed the sequential combinations in the control of viable bacteria and the antibiotic resistance in the subsequently formed biofilm.

Keywords: LED UV; chlorination; combined process; biofilm; drinking water; antibiotic resistance

1. Introduction

In the drinking water distribution system (DWDS), more than 90% of the biomass is found in biofilm, which would be a threat to the safety and aesthetics of drinking water: affecting taste and odour of water, reducing hydraulic efficiency, harbouring pathogens and promoting the propagation of antimicrobial resistance [1–4]. Controlling the biofilm formation in DWDS is therefore an important task for public health.

Disinfection is the most adopted precaution which inactivates the existing planktonic microorganisms to retard the growth of biofilm. Chlorination (Cl_2) is widely used as chlorine; it is an affordable chemical with persistent and broad biocidal effects such as damage to DNA, proteins, lipids, and other cell components [5]. However, chlorine shows a limited effect on chlorine-resistant microorganisms and may derive toxic by-products [6]. Ultraviolet (UV) is another practically affordable drinking water disinfection technology, and it is free of by-products [7,8]. Light-emitting diodes (LED) UV is a competitive light source for UV disinfection due to its safety, high efficiency, customised wavelength combination and small size [9,10]. However, UV irradiation inactivates the bacteria mainly via the dimerization of pyrimidine which could be repaired, and therefore lacks durative inactivation [11].

To overcome the drawbacks of a single process, the combined use of Cl_2 and UV has gained more attention in recent years. The simultaneous combination of UV and Cl_2 (UV/Cl) is an advanced oxidation process, where the yielded radicals were reported to enhance the inactivation of fungi [12], pathogens [13] and antibiotic resistance genes (ARGs) [14]. Sequential combinations, UV followed by Cl_2 (UV-Cl) or Cl_2 followed by UV (Cl-UV), were also more effective than the standalone process in ensuring biological safety in the water [14–19]. Although previous studies showed the benefits of combined UV and Cl_2 on the removals of waterborne microorganisms, only a few evaluated their impacts on the following biofilm formation. Some studies showed that UV-Cl effectively controlled *Escherichia coli* and iron recycling bacteria in biofilms compared to Cl_2 alone [20,21]. Liu et al. [22] found that UV-Cl was effective in inactivating waterborne opportunistic pathogens, while the opportunistic pathogens in biofilms were tolerant to both UV-Cl and Cl_2. Hence, the impacts of other combinations on biofilm formation as well as their influences on other biofilm characteristics, such as antibiotic resistance, need further investigation.

On the other hand, the use of combined UV and Cl_2 that primarily inactivates microorganisms will also affect the structure of natural organic matter (NOM) in water, which has an influence on the subsequently formed biofilm as well. UV irradiation limitedly affected the biodegradable dissolved organic carbon (BDOC) or assimilable organic carbon (AOC) in the solution [8,23]. However, Cl_2 and UV/Cl are inconsistently reported to reduce or increase the BDOC and AOC in waters [24,25], which depends on the water matrix and the operational conditions. Moreover, disinfection by-products generated in the combined processes differed from the standalone processes in terms of the diversity and the quantity [26]. Disinfection by-products are potential promotors for the propagation of antibiotic resistance [27,28]. The characteristics of NOM have a great impact on the subsequent biofilm formation in addition to the waterborne microorganisms [29,30]. Hence, it is important to explore the change of NOM during the combined UV and Cl_2 regarding its impact on the subsequent biofilm formation.

This study aims to assess the impacts of three combined LED UV and Cl_2 processes on the biofilm in DWDS. Two sequential combinations, UV-Cl and Cl-UV, and one simultaneous combination, UV/Cl, were adopted in a laboratory drinking water treatment system as the disinfection. The collected surface water samples were evaluated for the change of NOM characteristics in various treatment units before being fed into the biofilm reactor. Biofilm reactors were continuously run for 106 days, where the biofilms in different reactors were compared for the quantities of culturable bacteria, viable bacteria, extracellular polymeric substances (EPSs), culturable antibiotic resistant bacteria (ARB), selected ARGs and functional genes.

2. Materials and Methods

Water was sampled every two weeks from a local canal and underwent pre-treatment of coagulation/flocculation, settling and sand filtration in our laboratory (Figure S1). Samples were collected from the raw water mixing tank (Raw), effluents of the settling tank (ST) and effluents of the sand filter (SF) for further analyses.

The LED UV lamp has 40 LED chips (Klaran, Green Island, NY, USA) with the max yield at 265 nm (Figure S2). The average intensity of the LED UV lamp was measured by the ferrioxalate actinometry method [31], and the applied UV fluence in each process was controlled at 306 mJ/cm^2. Chlorine was diluted from commercial sodium hypochlorite solution (Sigma-Aldrich, Singapore), and its concentration was determined by an N, N-diethyl-p-phenylenediamine colourimetric method using a colourimeter (DR890, Hach, Loveland, CO, USA). In each process, chlorine was dosed at an initial concentration of 10 mg/L as Cl_2 and quenched by sodium thiosulfate. The water collected in pre-treatment or after disinfection was stored in the dark at 4 °C before further processing.

Four glass cylinders with microscopy slides glued to the acrylic lid were adopted as biofilm reactors (Figure S3). Biofilm reactors were continuously fed with water without disinfection (i.e., SF) and water treated with UV-Cl, Cl-UV and UV/Cl, respectively. The

hydraulic retention time was controlled at around 55 h, within the maximum reported water age (i.e., 72 h) in DWDS [32]. The solution inside the biofilm reactors was mixed continuously by a magnetic stirrer at 100 rpm. The whole biofilm reactors were wrapped with aluminium foil to mimic the dark condition in DWDS.

The changes of NOM in the pre-treatment and disinfection were monitored. Dissolved organic carbon (DOC) was measured by the high-temperature combustion method via a TOC analyser (TOC-L CPH, Shimazu, Kyoto, Japan). Total suspended solids (TSS) were obtained by quantifying the mass of the particles sustained by glass fibre filters. The content of chromophores was indicated by UV absorbance at 254 nm (UV254), which was measured by a UV-Vis spectrophotometer (DR6000, Hach, Loveland, CO, USA). A fluorescence spectrometer (Cary Eclipse, Agilent, Santa Clara, CA, USA) was adopted to monitor the change of fluorophores, where the obtained excitation–emission matrixes were further analysed by parallel factor analysis (PARAFAC) as detailed in Text S1 [33–35]. An LC-OCD analyser (Dr. Huber, Karlsruhe, Germany) was adopted to analyse the content of hydrophobic (HOC) and hydrophilic organic carbons of different molecular weights—biopolymers (>>20,000 g/mol), humic substances (500–1000 g/mol), building blocks (300–500 g/mol), lower molecular weight (LMW) neutrals and acids (<350 g/mol). To study the changes of functional groups by combined processes, NOMs were extracted by solid-phase extraction and freeze-dried before being analysed by Attenuated total reflectance–Fourier transform infrared spectroscopy (ATR–FTIR, VERTEX 70, Bruker, Bremen, Germany).

Biofilm was washed off by sonicating one microscope slide in 15 mL sterile deionised water. The culturable bacteria number was quantified by heterogeneous plate counting (HPC) using R2A agar plates (Sigma-Aldrich, Singapore) and incubated at 28 °C for 7 days. The EPS of biofilms from four reactors were quantified by bicinchoninic acid protein assay (Sigma-Aldrich, Singapore) and phenol-sulfuric acid method for protein and polysaccharides, respectively. A confocal laser scanning microscope (CLSM, Stellaris8, Leica, Wetzlar, Germany) was adopted to on-site characterise the biofilm structure. SYTO 9 and propidium iodide were used to stain nucleic acids in all cells and dead cells with damaged membranes, respectively (LIVE/DEAD kit, Thermo Fisher, Waltham, MA, USA). The CLSM data were further analysed by Imaris 9.9.0 and Image J.

The antibiotic resistance of biofilm was tested via quantification of culturable antibiotic resistance bacteria (ARB) and ARGs. For the ARB test, ampicillin (Amp), ciprofloxacin (Cip), tetracycline (Tet) and sulfamethoxazole/trimethoprim (SXT) mixture were spiked into R2A agar at 32 mg/L, 1 mg/L, 16 mg/L and 4/76 mg/L, respectively. The survival rate was adopted to indicate the resistance of bacteria and calculated via the following equation:

Survival = (Bacteria No. on antibiotics amended plate)/(Bacteria No. on pure plate).

In addition, the DNA of biofilm samples were extracted by SPINeasy DNA kit for soil (MP biomedicals, Irvine, CA, USA) and analysed by a real-time PCR (QuantStudio 1, Applied Biosystems, Waltham, MA, USA). The details of primers and real-time PCR settings are listed in Table S1 and Text S2 [36–39]. The amounts of ARGs were relatively quantified by the $2^{-\Delta\Delta Ct}$ method [40], where 16s rRNA was adopted as the internal control gene and SF was used as the control group (Text S3).

3. Results and Discussion

3.1. Degradation of Organics

As seen in Figure 1, although UV$_{254}$ and DOC of organics varied in a wide range in the raw water, they could be effectively reduced to 0.027 ± 0.003 cm^{-1} and 2.59 ± 0.67 mg/L, respectively, after the settling tank. Sand filtration showed limited removal of the dissolved organics while it lowered the total suspended solids to <1 mg/L (TSS, Figure S4). After sand filtration, three combined processes, UV-Cl, Cl-UV and UV/Cl, further decreased the average concentration of UV$_{254}$ by 11%, 17% and 33%, respectively. However, DOC was not further reduced by the combined processes. The effective reduction of UV$_{254}$ by UV/Cl could be attributed to the radicals, where reactive chlorine species were efficient in

destroying aromaticity but little contributed to the mineralization [41]. The slight increase of DOC values after combined processes might be due to the interference from chlorine during DOC measurement [42]. The calculated specific UV absorbance at 254 nm (SUVA$_{254}$) values of SF, UV-Cl, Cl-UV and UV/Cl were low (<2 L/mg·m), being 0.89, 0.61, 0.64 and 0.46 L/mg·m, respectively. It suggests that the majority of NOMs were hydrophilic [36].
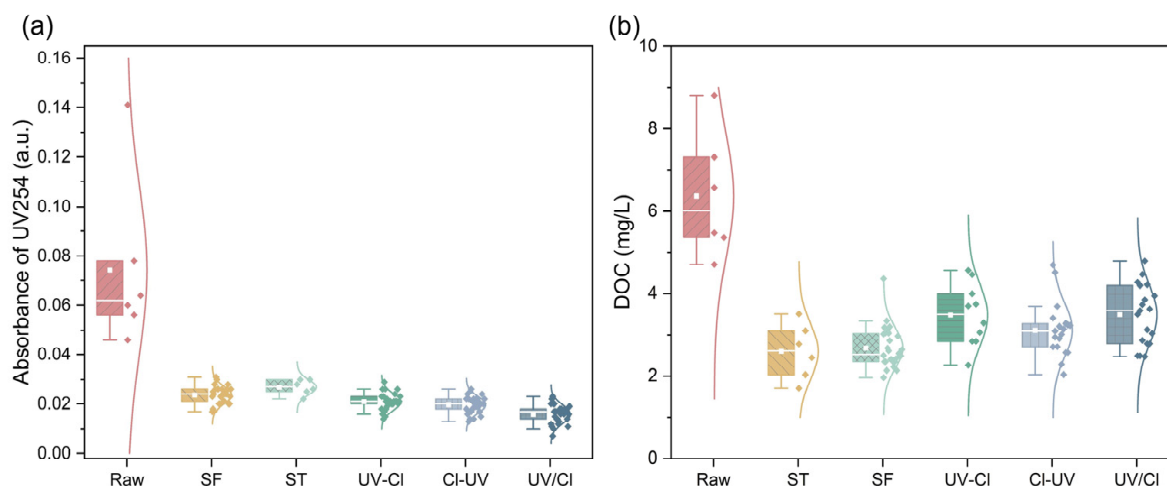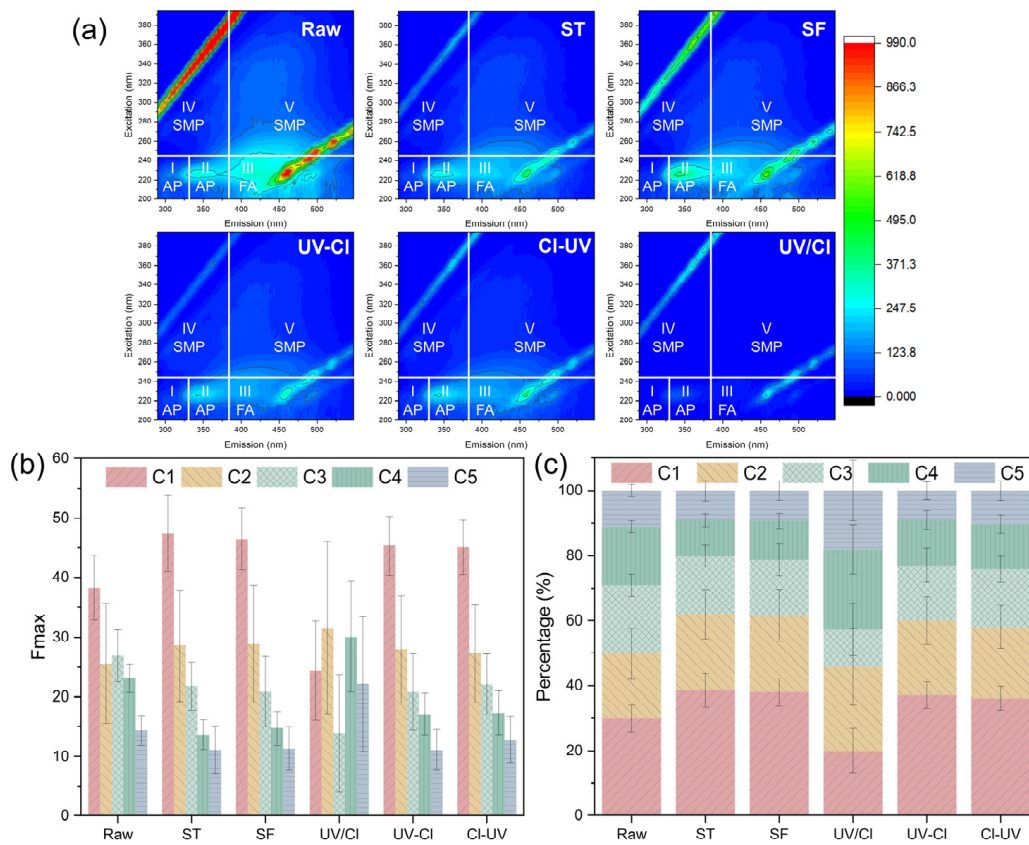

Figure 1. Changes of UV$_{254}$ (**a**) and DOC (**b**) in raw water (Raw), treated effluents from settling tank (ST), sand filtration (SF), UV-Cl, Cl-UV and UV/Cl.

The change of fluorescence EEM was in accordance with the change of UV$_{254}$, where the intensity of total fluorescence was continuously decreased in Raw, ST, SF and combined processes (Figure 2a). Amongst combined processes, UV/Cl was the most effective one to reduce fluorophores. PARAFAC analysis of fluorescence EEM derived five components—C1 to C5 refers to terrestrial humic-like, protein-like, humic-like, fulvic acid-like and tryptophan-like compounds, respectively (Figure S5, Table S2) [27,43–48]. As shown in Figure 2b,c, C3, C4 and C5 in raw water samples were reduced by coagulation/flocculation, while C1 was increased. After that, the relative contents of C1-C5 were maintained at similar levels in each unit except UV/Cl, where C1 and C3 were reduced with increased C4 and C5. The effective reduction of humic acid-like compounds (C1 and C3) in UV/Cl could be attributed to the generated radicals [49]. The increased fulvic acid-like compounds (C4) might be transformed from the reduction of the relatively large humic acid-like compounds. The tryptophan-like compounds (C5) in this study were similar to the reported one, which was strongly correlated with the biodegradability [50]. Hence, the increased C5 after UV/Cl implies the improved biodegradability. C2 are identified as synthetic organics compounds or anthropogenic compounds [51], which are relatively recalcitrant and changed slightly in the current study.

Molecular weight shifts of organics are shown in Figure 3. The relatively large molecules (biopolymer, humic substances and building blocks) were effectively removed and transformed into LMW molecules in the pre-treatment processes (Figure 3a). Compared to those of SF, HOC and LMW neutrals were increased after combined processes, and LMW neutrals were most abundant after UV-Cl, followed by UV/Cl (Figure 3b,c). The increased HOC could be attributed to the hydrophobic halogenated products formed from the reaction between NOM and chlorine [52]. Higher LMW compounds after combined processes imply that there were more abundant small organic molecules. Those small molecules were transformed from the larger molecules due to the breakdown by the combined processes [53].

Figure 2. Change of fluorescence EEM matrix (**a**), Fmax of PARAFAC components (**b**) and ratio of PARAFAC components (**c**) in raw water (Raw), treated effluents from settling tank (ST), sand filtration (SF), UV-Cl, Cl-UV and UV/Cl.
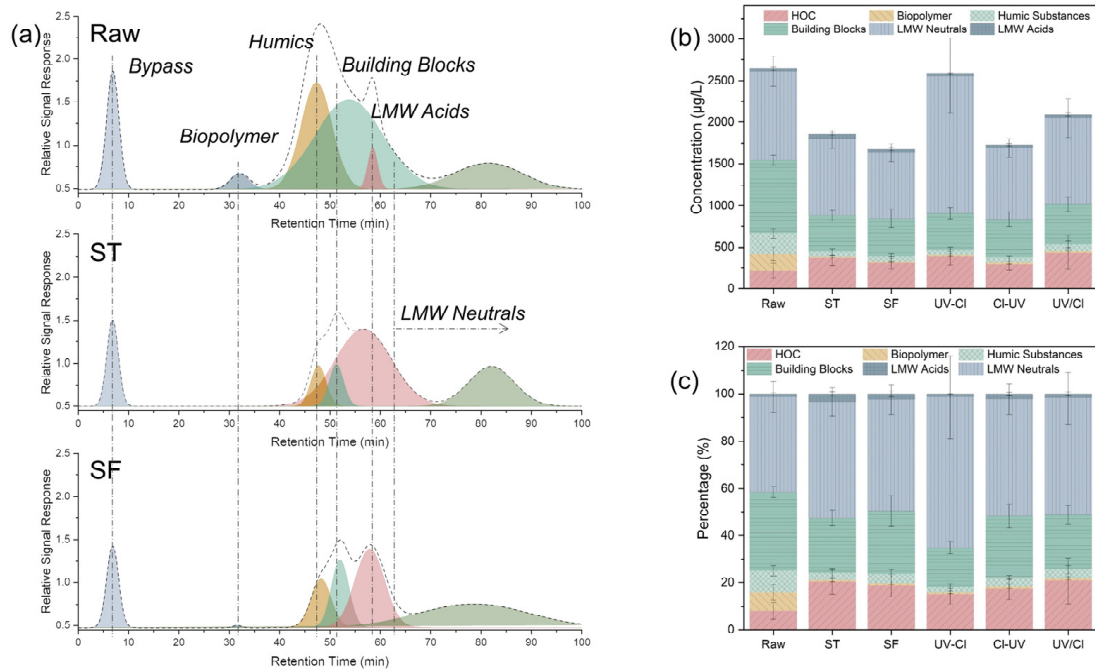

Figure 3. Shift of LC-OCD component diagram in pre-treatment processes (**a**); Change of LC-OCD components concentration (**b**) and percentage (**c**).

According to the results of ATR–FTIR (Figure S5, Text S4), the treatment by the combined processes did not make a significant change on the functional groups of NOM, except for the band at 1050 cm^{-1}. The increased intensities of bands at 1050 cm^{-1} after combined processes were associated with the increased C-O stretching, implying the possible formation of carbohydrates, alcohols and aliphatic ethers in combined processes [36,37].

Overall, the reduction of organics mainly occurred in pre-treatment units, while the combined processes could further alter the organics to be more accessible for microbial degradation. Specifically, the aromaticity of NOM could be reduced by the combined processes, as seen in the reduced UV$_{254}$ values (Figure 1a) and fluorescence intensities (Figure 2a). More LMW compounds were generated after combined processes, which might be some simple carbohydrates, alcohols or aliphatic ethers (Figure S5). Humic acid-like compounds were effectively reduced by UV/Cl, whereas fulvic acid-like compounds and proteins were increased. Organics with smaller molecular weight and higher hydrophilicity are more biodegradable compared to aromatic compounds [30]. Hence, the organics after the combined processes showed a higher affinity for the growth of microbes.

*3.2. Biofilm Formation and Antibiotic Resistance Control*

In the first trial of biofilm running, the solutions without disinfection and disinfected by combined processes of UV and Cl$_2$ were fed into the reactors. The culturable bacteria in the SF solution was 2.13×10^5 ($\pm 5.46 \times 10^4$) CFU/mL. Combined processes effectively inactivated the bacteria to below the detection limit (i.e., 300 CFU/mL), resulting in much lower levels of bacteria in the reactor solutions (Figure 4a). As seen in Figure 4b, the biofilm growths in reactors fed with the disinfected solution were inhibited until 21 days—when 5% seeding bacteria was added to disinfected reactors. With the seeds, the bacteria numbers in solution dramatically increased, and so did the numbers of biofilm bacteria in UV-Cl and Cl-UV (Figure 4b). The numbers of biofilm bacteria in UV-Cl and Cl-UV reached similar levels to those in SF (10^3–10^4 CFU/mL) within two weeks after seeding. The biofilm growth in UV/Cl was delayed compared to those in UV-Cl and Cl-UV, suggesting a less favourable environment in UV/Cl for biofilm growth. The results confirm that disinfection could inhibit the growth of biofilm effectively via the inactivation of bacteria. However, 5% seeding of bacteria resulted in similar levels of biofilm bacteria in the reactors, suggesting that insufficient disinfection is not better than no disinfection regarding biofilm control in a long-term perspective.
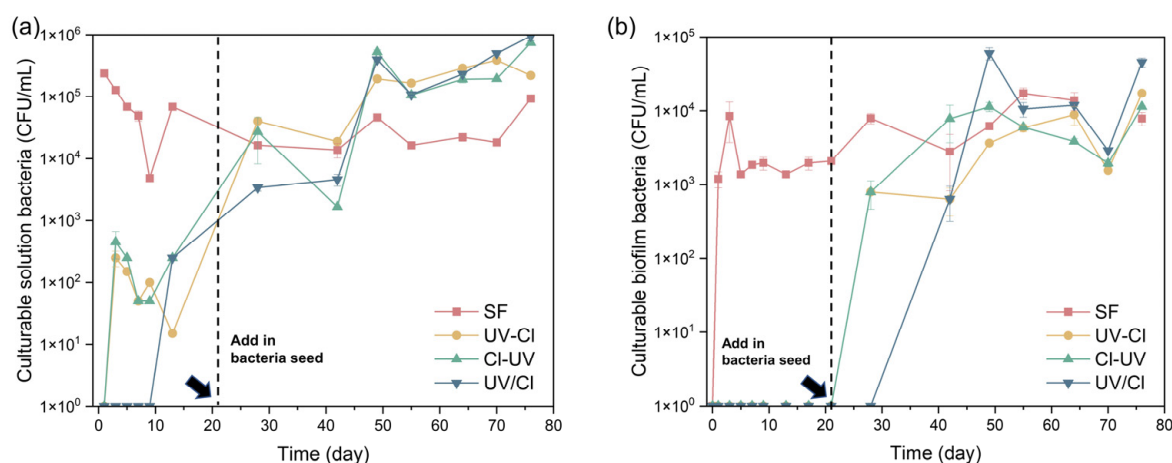
Figure 4. Culturable bacteria number in solution (**a**) and biofilm (**b**) in the reactors running without bacteria seed up to 21 days.

To further assess the impact of organics changed during disinfection on the biofilm growth, another trial of biofilm running was conducted, where 5% bacteria seed was added at the beginning (Figure 5). The numbers of solution bacteria were maintained in the range of 10^4–10^6 CFU/mL, with small differences amongst reactors (Figure 5a). Biofilm in each

reactor grew similarly fast in the first 10 days. After that, biofilm bacteria in SF stabilized at around 10^4 CFU/mL, while the numbers of biofilm bacteria in UV-Cl, Cl-UV and UV/Cl were increased continuously to reach 10^5 CFU/mL. The inconsistency of culturable bacteria in solution and biofilm was observed before, where not only the number of bacteria but also their antibiotic resistance was different [54]. The varied biofilm bacteria numbers in the bioreactors indicate that water treated by combined processes was more favourable for the culturable biofilm bacteria to grow, which could be attributed to the more available biodegradable organics after the combined processes.
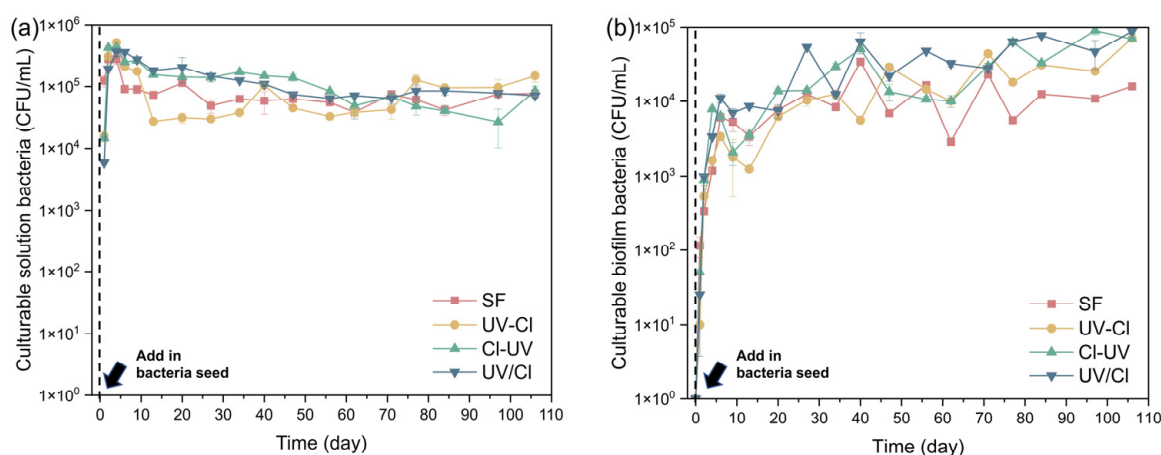

Figure 5. Culturable bacteria number in solution (**a**) and biofilm (**b**) in the reactors running with bacteria seed from day 1. Reactors were running for 106 days.

However, bacteria culturable by R2A medium count for <3% of the total bacteria [55,56]. Viable but non-culturable (VBNC) bacteria pose potential risks since they could display pathogenicity and resuscitate under appropriate conditions [17]. Therefore, biofilm bacteria were stained and in situ observed under CLSM (Figure 6). The quantity of biofilm bacteria observed on CLSM (Figure 6a) showed contrary results to the culturable bacteria results (Figure 5a), where the highest intensity was observed in SF, followed by Cl-UV, UV-Cl, and least bacteria were seen in UV/Cl. Compared to the bacteria in SF, considerate amounts of bacteria observed in UV-Cl, Cl-UV and UV/Cl were damaged or dead (Figure 6b,c). The CLSM results suggest that disinfection by combined processes could suppress the viable bacteria in biofilm, and UV/Cl is the most effective one. The contents of proteins in the biofilm EPS were similar amongst reactors, which were lower than the contents of EPS polysaccharides (Figure S7).

The antimicrobial resistance in the biofilm was further examined. The survival rates of biofilm bacteria to Amp, Cip, Tet and SXT were presented to indicate the content of culturable ARB (Figure 7a). Biofilm bacteria from all reactors showed high survival rates in the presence of Amp (55.5–87.6%), implying the presence of abundant Amp-resistant bacteria. On the contrary, biofilm bacteria were not resistant to Tet in all reactors (<10%). Biofilm bacteria in the control reactor showed high resistance to Cip (49.9%), and the resistance was decreased in reactors fed with disinfected solution, with survival rates of 27.7%, 16.0% and 10.8% in UV-Cl, Cl-UV and UV/Cl reactors, respectively. The resistance to SXT was dramatically reduced in biofilm bacteria in UV/Cl (16.8%) compared to those in other reactors (43.6–55.0%). These results indicate that disinfection by combined processes could help reduce the contents of Cip-resistant ARB in the biofilm, and UV/Cl could further reduce the SXT-resistant ARB.
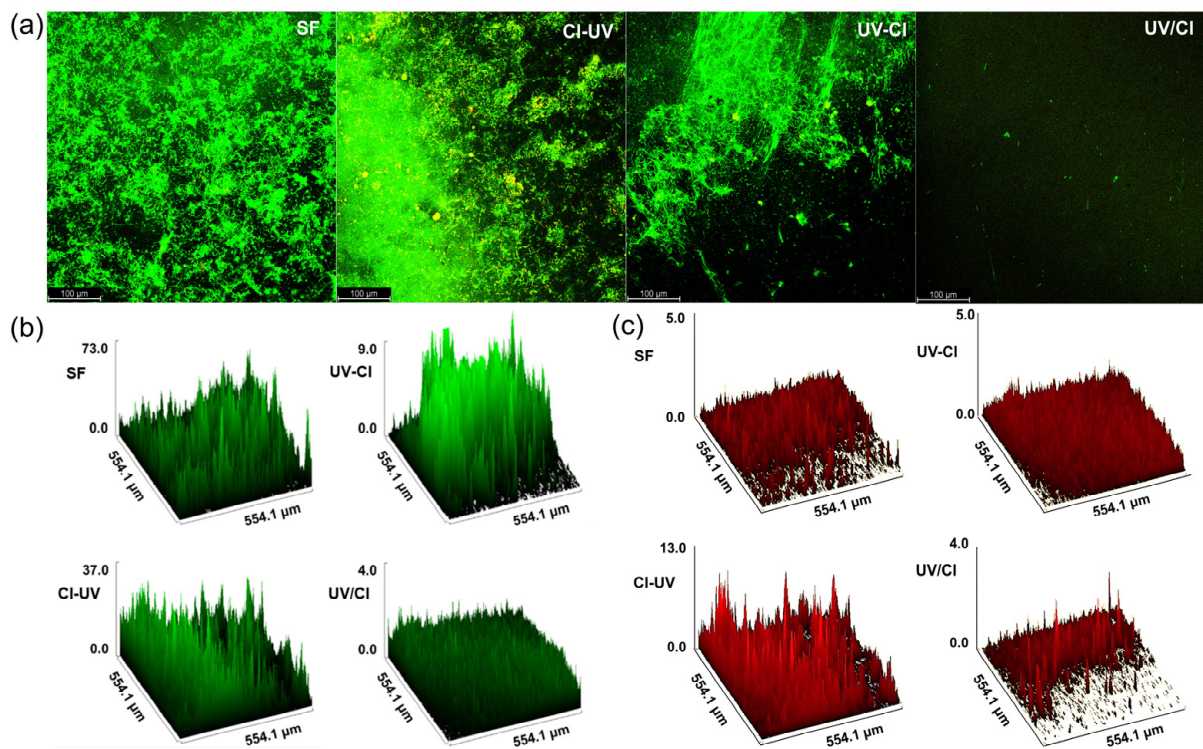
Figure 6. CLSM micrograph of biofilm grown in waters from SF, UV-Cl, Cl-UV and UV/Cl. Projected upper view of the biofilm (**a**); Estimated total bacteria intensity of surface plot of the biofilm (**b**); Estimated dead bacteria intensity of surface plot of the biofilm (**c**).
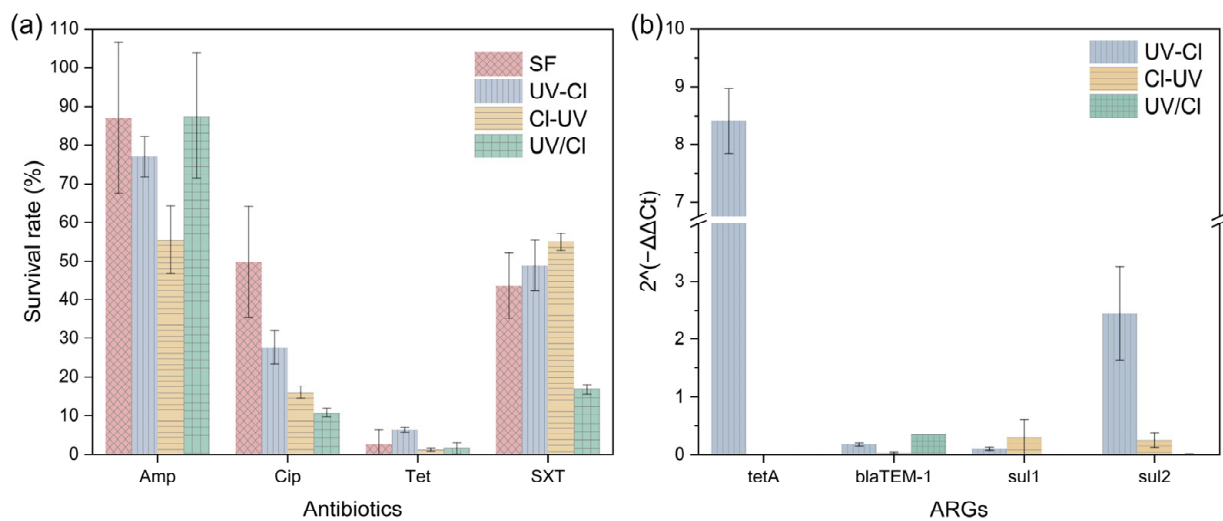
Figure 7. Percentage of culturable ARB (**a**) and relative abundance of ARGs (**b**) in biofilm.

Four out of seven target genes were detected in biofilm samples and relatively quantified (Figure 7b), while the functional genes (*intl1*, *intl2*) and other ARGs (i.e., *oqxB*, *mexB*, *adeA*, *qnrS*) were below detection limits in all reactors. Generally, the contents of ARGs in the biofilm could be reduced by the combined processes with the majority of calculated $2^{-\Delta\Delta Ct} < 1$. However, the contents of *tetA* and *sul2* in the biofilm were increased after UV-Cl, implying a potential risk of enriching ARGs. Some results of ARGs could explain the observed culturable ARB (Figure 7a): the content of *tetA* in UV-Cl was much higher compared to that of SF, which is consistent with the higher Tet-resistance of biofilm bacteria in UV-Cl (6.3%) than those in other reactors (<2.5%). The sulfamethoxazole resistance genes, *sul1* and

sul2, were nearly non-existing in the UV/Cl reactor compared to those in SF, explaining its low biofilm bacteria resistance toward SXT (Figure 7a). UV/Cl is reported to more efficiently reduce *sul1* gene compared to standalone UV or Cl_2 for waterborne bacteria, which might result in the lower *sul1* genes in the biofilm fed with UV/Cl treated water in the current study [57]. However, the high content of *sul2* did not lead to an increased culturable SXT-resistance ARB in UV-Cl and ARGs with $2^{-\Delta\Delta Ct} < 1$ did not help reduce the culturable ARB compared to SF, which might indicate the existence of antibiotic resistance in VBNC bacteria. The ARGs carried by VBNC bacteria were reported to retain a certain level of plasmid gene transfer efficiency [58] and equip bacteria with resistance to antibiotics [27]. The effectiveness of UV/Cl has been reported in the water regarding the inactivation of culturable bacteria, VBNC and pathogens as well as the removals of ARGs and mobile genetic elements [59]. Nonetheless, ARGs could not be completely eliminated from the water, coherent with our detected antibiotic resistance in the subsequently formed biofilm. Our results of ARB and ARGs on biofilm reveal that combined processes help reduce the antibiotic resistance in the subsequently formed biofilm, where UV/Cl outperforms the other two combinations regarding the simultaneous control of ARB and ARGs.

4. Conclusions

This study investigated the influences of UV-Cl, Cl-UV and UV/Cl as disinfection on the subsequent formation of biofilm. Three combined processes effectively inactivated the culturable bacteria, and further altered the characteristics of NOM after the pre-treatment process (i.e., coagulation/flocculation, settling and sand filtration). After the combined processes, NOM consisted of more available small molecules and less aromaticity, implying an increased biodegradability. It may enhance the growth of culturable bacteria in the biofilm, where the culturable biofilm bacteria in the reactors fed with disinfected solutions reached 10^5 CFU/mL in 106 days, higher than that in the control reactor without disinfection (10^4 CFU/mL). However, the viable biofilm bacteria observed by CLSM were fewer after the combined process, especially after UV/Cl. Combined processes suppressed the culturable Cip-resistant ARB in biofilm, with the survival rates reduced from 49.9% in the control reactor to 27.7%, 16.0% and 10.8% in UV-Cl, Cl-UV and UV/Cl, respectively. The survival rate of SXT-resistant biofilm ARB in UV/Cl (16.8%) was lowest compared to that in other reactors (43.6–55.0%), consistent with the little *sul1* and *sul2* detected in UV/Cl. Although combined processes reduced the contents of most detected ARGs (i.e., *blaTEM-1*, *tetA*, *sul1* and *sul2*), UV-Cl showed the potential to enrich *tetA* and *sul2* in the subsequently formed biofilm. This study showed that UV/Cl would be alternative disinfection in drinking water treatment to help control the viable biofilm bacteria and the antibiotic resistance in the biofilm.

Supplementary Materials: The following supporting information can be downloaded at: https://www.mdpi.com/article/10.3390/w14223643/s1, Figure S1: Illustration of pre-treatment processes; Figure S2: Schematic diagram of LED-UV lamp from top view (a) and side view (b); Figure S3: Schematic diagram of biofilm reactor; Figure S4: Removal of total suspended solids (TSS) in pretreatment processes; Figure S5: Identified EEM-PARAFAC components in water samples (C1-C5) and their spectral loadings; Figure S6: FTIR spectrum of organics after sand filtration (SF), UV-Cl, Cl-UV and UV/Cl; Figure S7: Polysaccharide and protein in extracellular polymeric substances of biofilm; Table S1: Details of primers used in this study; Table S2: PARAFAC components from 5-component model; Text S1: Parallel factor (PARAFAC) analysis of fluorescence excitation-emission matrix; Text S2: Detection of target genes by real-time PCR; Text S3: Detection and quantification of target ARGs; Text S4: Analysis of ATR–FTIR results.

Author Contributions: Conceptualization, Y.C.; methodology, Y.C. and T.Y.C.; software, Y.L.; validation, Y.L. and S.Y.; formal analysis, Y.C. and Y.L.; investigation, Y.L., S.Y. and T.Y.C.; resources, J.H.; data curation, Y.C. and Y.L.; writing—original draft preparation, Y.C.; writing—review and editing, Y.L., X.Z. and J.H.; visualization, Y.L.; supervision, X.Z. and J.H.; project administration, J.H.; funding acquisition, J.H. All authors have read and agreed to the published version of the manuscript.

Conflicts of Interest: The authors declare no conflict of interest.

References

1. Chen, J.; Li, W.; Zhang, J.; Qi, W.; Li, Y.; Chen, S.; Zhou, W. Prevalence of Antibiotic Resistance Genes in Drinking Water and Biofilms: The Correlation with the Microbial Community and Opportunistic Pathogens. *Chemosphere* **2020**, *259*, 127483. [CrossRef] [PubMed]
2. Waak, M.B.; LaPara, T.M.; Hallé, C.; Hozalski, R.M. Occurrence of Legionella Spp. in Water-Main Biofilms from Two Drinking Water Distribution Systems. *Environ. Sci. Technol.* **2018**, *52*, 7630–7639. [CrossRef]
3. Liu, G.; Zhang, Y.; Knibbe, W.-J.; Feng, C.; Liu, W.; Medema, G.; van der Meer, W. Potential Impacts of Changing Supply-Water Quality on Drinking Water Distribution: A Review. *Water Res.* **2017**, *116*, 135–148. [CrossRef]
4. Wingender, J.; Flemming, H.-C. Biofilms in Drinking Water and Their Role as Reservoir for Pathogens. *Int. J. Hyg. Environ. Health* **2011**, *214*, 417–423. [CrossRef] [PubMed]
5. Douterelo, I.; Calero-Preciado, C.; Soria-Carrasco, V.; Boxall, J.B. Whole Metagenome Sequencing of Chlorinated Drinking Water Distribution Systems. *Environ. Sci. Water Res. Technol.* **2018**, *4*, 2080–2091. [CrossRef]
6. Zheng, J.; Su, C.; Zhou, J.; Xu, L.; Qian, Y.; Chen, H. Effects and Mechanisms of Ultraviolet, Chlorination, and Ozone Disinfection on Antibiotic Resistance Genes in Secondary Effluents of Municipal Wastewater Treatment Plants. *Chem. Eng. J.* **2017**, *317*, 309–316. [CrossRef]
7. Li, X.; Cai, M.; Wang, L.; Niu, F.; Yang, D.; Zhang, G. Evaluation Survey of Microbial Disinfection Methods in UV-LED Water Treatment Systems. *Sci. Total Environ.* **2019**, *659*, 1415–1427. [CrossRef] [PubMed]
8. Choi, Y.; Choi, Y.-J. The Effects of UV Disinfection on Drinking Water Quality in Distribution Systems. *Water Res.* **2010**, *44*, 115–122. [CrossRef] [PubMed]
9. Luo, X.; Zhang, B.; Lu, Y.; Mei, Y.; Shen, L. Advances in Application of Ultraviolet Irradiation for Biofilm Control in Water and Wastewater Infrastructure. *J. Hazard. Mater.* **2022**, *421*, 126682. [CrossRef] [PubMed]
10. Torkzadeh, H.; Cates, E.L. Biofilm Growth under Continuous UVC Irradiation: Quantitative Effects of Growth Conditions and Growth Time on Intensity Response Parameters. *Water Res.* **2021**, *206*, 117747. [CrossRef]
11. Ghosh, S.; Chen, Y.; Hu, J. Application of UVC and UVC Based Advanced Disinfection Technologies for the Inactivation of Antibiotic Resistance Genes and Elimination of Horizontal Gene Transfer Activities: Opportunities and Challenges. *Chem. Eng. J.* **2022**, *450*, 138234. [CrossRef]
12. Wan, Q.; Wen, G.; Cao, R.; Zhao, H.; Xu, X.; Xia, Y.; Wu, G.; Lin, W.; Wang, J.; Huang, T. Simultaneously Enhance the Inactivation and Inhibit the Photoreactivation of Fungal Spores by the Combination of UV-LEDs and Chlorine: Kinetics and Mechanisms. *Water Res.* **2020**, *184*, 116143. [CrossRef] [PubMed]
13. Wang, L.; Ye, C.; Guo, L.; Chen, C.; Kong, X.; Chen, Y.; Shu, L.; Wang, P.; Yu, X.; Fang, J. Assessment of the UV/Chlorine Process in the Disinfection of Pseudomonas Aeruginosa: Efficiency and Mechanism. *Environ. Sci. Technol.* **2021**, *55*, 9221–9230. [CrossRef]
14. Liu, X.; Hu, J.Y. Effect of DNA Sizes and Reactive Oxygen Species on Degradation of Sulphonamide Resistance Sul1 Genes by Combined UV/Free Chlorine Processes. *J. Hazard. Mater.* **2020**, *392*, 122283. [CrossRef] [PubMed]
15. Forsyth, J.E.; Zhou, P.; Mao, Q.; Asato, S.S.; Meschke, J.S.; Dodd, M.C. Enhanced Inactivation of Bacillus Subtilis Spores during Solar Photolysis of Free Available Chlorine. *Environ. Sci. Technol.* **2013**, *47*, 12976–12984. [CrossRef]
16. Wang, Z.; Hessler, C.M.; Xue, Z.; Seo, Y. The Role of Extracellular Polymeric Substances on the Sorption of Natural Organic Matter. *Water Res.* **2012**, *46*, 1052–1060. [CrossRef]
17. Zhang, Y.; Zhuang, Y.; Geng, J.; Ren, H.; Zhang, Y.; Ding, L.; Xu, K. Inactivation of Antibiotic Resistance Genes in Municipal Wastewater Effluent by Chlorination and Sequential UV/Chlorination Disinfection. *Sci. Total Environ.* **2015**, *512–513*, 125–132. [CrossRef]
18. Zyara, A.M.; Torvinen, E.; Veijalainen, A.-M.; Heinonen-Tanski, H. The Effect of UV and Combined Chlorine/UV Treatment on Coliphages in Drinking Water Disinfection. *Water* **2016**, *8*, 130. [CrossRef]
19. Shekhawat, S.S.; Kulshreshtha, N.M.; Vivekanand, V.; Gupta, A.B. Impact of Combined Chlorine and UV Technology on the Bacterial Diversity, Antibiotic Resistance Genes and Disinfection by-Products in Treated Sewage. *Bioresour. Technol.* **2021**, *339*, 125615. [CrossRef]
20. Murphy, H.M.; Payne, S.J.; Gagnon, G.A. Sequential UV- and Chlorine-Based Disinfection to Mitigate *Escherichia coli* in Drinking Water Biofilms. *Water Res.* **2008**, *42*, 2083–2092. [CrossRef]
21. Zhu, Y.; Chen, L.; Xiao, H.; Shen, F.; Deng, S.; Zhang, S.; He, J.; Song, C.; Wang, X.; Zhang, J.; et al. Effects of Disinfection Efficiency on Microbial Communities and Corrosion Processes in Drinking Water Distribution Systems Simulated with Actual Running Conditions. *J. Environ. Sci.* **2020**, *88*, 273–282. [CrossRef] [PubMed]
22. Liu, L.; Xing, X.; Hu, C.; Wang, H.; Lyu, L. Effect of Sequential UV/Free Chlorine Disinfection on Opportunistic Pathogens and Microbial Community Structure in Simulated Drinking Water Distribution Systems. *Chemosphere* **2019**, *219*, 971–980. [CrossRef] [PubMed]

23. Shaw, J.P.; Malley Jr., J.P.; Willoughby, S.A. Effects of UV Irradiation on Organic Matter. *J. AWWA* **2000**, *92*, 157–167. [CrossRef]
24. Rosińska, A.; Rakocz, K. The Influence UV/Chlorination Process on Changes of Biodegradable Fraction in Water. *J. Clean. Prod.* **2021**, *278*, 123947. [CrossRef]
25. Huang, G.; Ng, T.-W.; Chen, H.; Chow, A.T.; Liu, S.; Wong, P.K. Formation of Assimilable Organic Carbon (AOC) during Drinking Water Disinfection: A Microbiological Prospect of Disinfection Byproducts. *Environ. Int.* **2020**, *135*, 105389. [CrossRef] [PubMed]
26. Chen, Y.; Jafari, I.; Zhong, Y.; Chee, M.J.; Hu, J. Degradation of Organics and Formation of DBPs in the Combined LED-UV and Chlorine Processes: Effects of Water Matrix and Fluorescence Analysis. *Sci. Total Environ.* **2022**, *846*, 157454. [CrossRef]
27. Amarasiri, M.; Sano, D.; Suzuki, S. Understanding Human Health Risks Caused by Antibiotic Resistant Bacteria (ARB) and Antibiotic Resistance Genes (ARG) in Water Environments: Current Knowledge and Questions to Be Answered. *Crit. Rev. Environ. Sci. Technol.* **2020**, *50*, 2016–2059. [CrossRef]
28. Lv, L.; Jiang, T.; Zhang, S.; Yu, X. Exposure to Mutagenic Disinfection Byproducts Leads to Increase of Antibiotic Resistance in Pseudomonas Aeruginosa. *Environ. Sci. Technol.* **2014**, *48*, 8188–8195. [CrossRef]
29. Wang, M.; Ateia, M.; Awfa, D.; Yoshimura, C. Regrowth of Bacteria after Light-Based Disinfection—What We Know and Where We Go from Here. *Chemosphere* **2021**, *268*, 128850. [CrossRef]
30. Liu, S.; Gunawan, C.; Barraud, N.; Rice, S.A.; Harry, E.J.; Amal, R. Understanding, Monitoring, and Controlling Biofilm Growth in Drinking Water Distribution Systems. *Environ. Sci. Technol.* **2016**, *50*, 8954–8976. [CrossRef]
31. Bolton, J.R.; Stefan, M.I.; Shaw, P.-S.; Lykke, K.R. Determination of the Quantum Yields of the Potassium Ferrioxalate and Potassium Iodide–Iodate Actinometers and a Method for the Calibration of Radiometer Detectors. *J. Photochem. Photobiol. A Chem.* **2011**, *222*, 166–169. [CrossRef]
32. AWWA. AWWARF Water Industry Database: Utility Profiles. In *American Water Works Association*; American Water Works Association Research Foundation: Denver, CO, USA, 1992.
33. Micó, P.; García-Ballesteros, S.; Mora, M.; Vicente, R.; Amat, A.M.; Arques, A. EEMlab: A Graphical User-Friendly Interface for Fluorimetry Experiments Based on the DrEEM Toolbox. *Chemom. Intell. Lab. Syst.* **2019**, *188*, 6–13. [CrossRef]
34. Murphy, K.R.; Stedmon, C.A.; Graeber, D.; Bro, R. Fluorescence Spectroscopy and Multi-Way Techniques. PARAFAC. *Anal. Methods* **2013**, *5*, 6557–6566. [CrossRef]
35. Murphy, K.R.; Stedmon, C.A.; Wenig, P.; Bro, R. OpenFluor—An Online Spectral Library of Auto-Fluorescence by Organic Compounds in the Environment. *Anal. Methods* **2014**, *6*, 658–661. [CrossRef]
36. Wang, H.; Zhu, Y.; Hu, C.; Hu, X. Treatment of NOM Fractions of Reservoir Sediments: Effect of UV and Chlorination on Formation of DBPs. *Sep. Purif. Technol.* **2015**, *154*, 228–235. [CrossRef]
37. Rodríguez, F.J.; Núñez, L.A. Characterization of Aquatic Humic Substances. *Water Environ. J.* **2011**, *25*, 163–170. [CrossRef]
38. Zhou, S.; Shao, Y.; Gao, N.; Deng, Y.; Li, L.; Deng, J.; Tan, C. Characterization of Algal Organic Matters of Microcystis Aeruginosa: Biodegradability, DBP Formation and Membrane Fouling Potential. *Water Res.* **2014**, *52*, 199–207. [CrossRef]
39. Platikanov, S.; Tauler, R.; Rodrigues, P.M.S.M.; Antunes, M.C.G.; Pereira, D.; Esteves da Silva, J.C.G. Factorial Analysis of the Trihalomethane Formation in the Reaction of Colloidal, Hydrophobic, and Transphilic Fractions of DOM with Free Chlorine. *Environ. Sci. Pollut. Res.* **2010**, *17*, 1389–1400. [CrossRef]
40. Livak, K.J.; Schmittgen, T.D. Analysis of Relative Gene Expression Data Using Real-Time Quantitative PCR and the $2^{-\Delta\Delta CT}$ Method. *Methods* **2001**, *25*, 402–408. [CrossRef]
41. Chen, Y.; Li, S.; Hu, J. Photoelectrocatalytic Degradation of Organics and Formation of Disinfection Byproducts in Reverse Osmosis Concentrate. *Water Res.* **2020**, *168*, 115105. [CrossRef]
42. Hu, X. Formation Potential of Disinfection By-Products after Coagulation of Algal Matters. Master's thesis, The University of Western Ontario, London, ON, Canada, 2016.
43. Murphy, K.R.; Hambly, A.; Singh, S.; Henderson, R.K.; Baker, A.; Stuetz, R.; Khan, S.J. Organic Matter Fluorescence in Municipal Water Recycling Schemes: Toward a Unified PARAFAC Model. *Environ. Sci. Technol.* **2011**, *45*, 2909–2916. [CrossRef] [PubMed]
44. Bianchi, T.S.; Osburn, C.; Shields, M.R.; Yvon-Lewis, S.; Young, J.; Guo, L.; Zhou, Z. Deepwater Horizon Oil in Gulf of Mexico Waters after 2 Years: Transformation into the Dissolved Organic Matter Pool. *Environ. Sci. Technol.* **2014**, *48*, 9288–9297. [CrossRef] [PubMed]
45. Lin, H.; Guo, L. Variations in Colloidal DOM Composition with Molecular Weight within Individual Water Samples as Characterized by Flow Field-Flow Fractionation and EEM-PARAFAC Analysis. *Environ. Sci. Technol.* **2020**, *54*, 1657–1667. [CrossRef] [PubMed]
46. Stedmon, C.A.; Thomas, D.N.; Granskog, M.; Kaartokallio, H.; Papadimitriou, S.; Kuosa, H. Characteristics of Dissolved Organic Matter in Baltic Coastal Sea Ice: Allochthonous or Autochthonous Origins? *Environ. Sci. Technol.* **2007**, *41*, 7273–7279. [CrossRef]
47. Yamashita, Y.; Boyer, J.N.; Jaffé, R. Evaluating the Distribution of Terrestrial Dissolved Organic Matter in a Complex Coastal Ecosystem Using Fluorescence Spectroscopy. *Cont. Shelf Res.* **2013**, *66*, 136–144. [CrossRef]
48. Chen, W.; Westerhoff, P.; Leenheer, J.A.; Booksh, K. Fluorescence Excitation−Emission Matrix Regional Integration to Quantify Spectra for Dissolved Organic Matter. *Environ. Sci. Technol.* **2003**, *37*, 5701–5710. [CrossRef]
49. Bulman, D.M.; Remucal, C.K. Role of Reactive Halogen Species in Disinfection Byproduct Formation during Chlorine Photolysis. *Environ. Sci. Technol.* **2020**, *54*, 9629–9639. [CrossRef]
50. Yang, L.; Shin, H.-S.; Hur, J. Estimating the Concentration and Biodegradability of Organic Matter in 22 Wastewater Treatment Plants Using Fluorescence Excitation Emission Matrices and Parallel Factor Analysis. *Sensors* **2014**, *14*, 1771–1786. [CrossRef]

51. Yu, H.; Qu, F.; Sun, L.; Liang, H.; Han, Z.; Chang, H.; Shao, S.; Li, G. Relationship between Soluble Microbial Products (SMP) and Effluent Organic Matter (EfOM): Characterized by Fluorescence Excitation Emission Matrix Coupled with Parallel Factor Analysis. *Chemosphere* **2015**, *121*, 101–109. [CrossRef]

52. Wan, Y.; Xie, P.; Wang, Z.; Ding, J.; Wang, J.; Wang, S.; Wiesner, M.R. Comparative Study on the Pretreatment of Algae-Laden Water by UV/Persulfate, UV/Chlorine, and UV/H2O2: Variation of Characteristics and Alleviation of Ultrafiltration Membrane Fouling. *Water Res.* **2019**, *158*, 213–226. [CrossRef]

53. Wang, W.-L.; Zhang, X.; Wu, Q.-Y.; Du, Y.; Hu, H.-Y. Degradation of Natural Organic Matter by UV/Chlorine Oxidation: Molecular Decomposition, Formation of Oxidation Byproducts and Cytotoxicity. *Water Res.* **2017**, *124*, 251–258. [CrossRef] [PubMed]

54. Tsvetanova, Z.; Tsvetkova, I.; Najdenski, H. Antimicrobial Resistance of Heterotrophic Bacteria in Drinking Water-Associated Biofilms. *Water* **2022**, *14*, 944. [CrossRef]

55. Sim[otilde]es, L.C.; Azevedo, N.; Pacheco, A.; Keevil, C.W.; Vieira, M.J. Drinking Water Biofilm Assessment of Total and Culturable Bacteria under Different Operating Conditions. *Biofouling* **2006**, *22*, 91–99. [CrossRef] [PubMed]

56. Bernard, L.; Schäfer, H.; Joux, F.; Courties, C.; Muyzer, G.; Lebaron, P. Genetic Diversity of Total, Active and Culturable Marine Bacteria in Coastal Seawater. *Aquat. Microb. Ecol.* **2000**, *23*, 1–11. [CrossRef]

57. Zhang, T.; Hu, Y.; Jiang, L.; Yao, S.; Lin, K.; Zhou, Y.; Cui, C. Removal of Antibiotic Resistance Genes and Control of Horizontal Transfer Risk by UV, Chlorination and UV/Chlorination Treatments of Drinking Water. *Chem. Eng. J.* **2019**, *358*, 589–597. [CrossRef]

58. Salcedo, D.E.; Kim, S. Fate of Tetracycline Resistance in Synthetic Livestock Carcass Leachate for Two Years. *J. Environ. Manag.* **2017**, *187*, 220–228. [CrossRef]

59. Ye, C.; Chen, Y.; Feng, L.; Wan, K.; Li, J.; Feng, M.; Yu, X. Effect of the Ultraviolet/Chlorine Process on Microbial Community Structure, Typical Pathogens, and Antibiotic Resistance Genes in Reclaimed Water. *Front. Environ. Sci. Eng.* **2021**, *16*, 100. [CrossRef]